PASJ: Publ. Astron. Soc. Japan **45**, 179–189 (1993)

Detection of SiO and H_2O Masers in Galactic Bulge Sources

Yoshikazu NAKADA
Kiso Observatory, Institute of Astronomy, the University of Tokyo, Mitake, Kiso, Nagano 397-01

Takashi ONAKA and Issei YAMAMURA
Department of Astronomy, the University of Tokyo, Bunkyo-ku, Tokyo 113

Shuji DEGUCHI and Nobuharu UKITA
Nobeyama Radio Observatory, Minamimaki-mura, Minamisaku-gun, Nagano 384-13*
and
Hideyuki IZUMIURA
Department of Astronomy and Earth Science, Tokyo Gakugei University, Koganei, Tokyo 184

(Received 1992 May 22; accepted 1992 September 21)

Abstract

We present the results of the first survey of Galactic bulge objects by the SiO $J = 1$–0 ($v = 1$ and 2) and H_2O 6_{16}–5_{23} transitions. The sources were selected from the IRAS Point Source Catalog with 12 μm intensity less than 14 Jy and colors, $(\log[f_\nu(25)/f_\nu(12)])$, between 0 and 0.2, extracting dust enshrouded objects at a distance of 8 kpc. Twenty three IRAS sources were observed; SiO masers were detected in fifteen objects, and H_2O in six sources. The overall properties of maser emission for bulge IRAS sources indicate that they are low-mass stars as optical Mira variables. Measurements of the SiO $J = 1$–0, $v = 1$ and 2 lines indicate that the intensity ratio of the $v = 2$ to $v = 1$ lines is nearly unity. The high detection rate of SiO masers in bulge objects seems to be due to the high sensitivity of the telescope used. The radial velocities of the maser lines reveal the average rotation of the bulge with a rotation velocity of 10 km s^{-1} deg^{-1}.

Key words: Galactic bulge — Galactic rotation — Masers

1. Introduction

The Galactic bulge, as mapped by IRAS, is a box-shaped stellar system extending over 20° around the galactic center. Bulge sources in the IRAS point Source Catalog are recorded as faint and red sources. More than 2500 IRAS bulge sources are believed to be stars in the final stage of stellar evolution and thus having active mass ejection (Habing 1985). They are aged low-mass objects with a mass of probably less than 1 $M_\odot$ and with a distance of 7–8 kpc (Feast 1987; Reid et al. 1988). Observations at near-infrared wavelengths (Frogel 1988) seem to indicate that the bulge sources exhibit a different color-color relation from that of disk sources. Although radio surveys by OH 1612 MHz in this region have been carried out by te Lintel-Hekkert et al. (1990), the nature of bulge OH/IR sources has not yet been fully understood.

We have carried out an extensive SiO and H_2O maser survey for bulge IRAS sources; this paper presents the first result of the survey. The primary aim of our study was to understand the basic nature of SiO masers of bulge sources and to clarify the circumstellar/atmospheric conditions of the mass-losing stars in the bulge. The excitation mechanism of SiO masers is disputed (e.g., Langer and Watson 1984). The apparent correlation of the maser intensity with the infrared continuum flux (Bujarrabal et al. 1987) seems to favor infrared pumping. Shock waves also seem to play an important role in a collisional pumping mechanism (Heske 1987). In this study, we surveyed IRAS sources with color $(\log[f_\nu(25)/f_\nu(12)])$, between 0 and 0.2, since they are normally strong maser emitters.

The kinematics of Galactic bulge sources was another issue. The systematic rotation of the Galactic bulge has been investigated for planetary nebulae (Minkowski 1964), Mira variables (Feast et al. 1980), RR Lyrae stars (Gratton 1987), and M stars (Mould 1983). These observations were made for stars in Baade's and other optical windows; it was concluded that the bulge rotation rate is small (about 10 km s^{-1} deg^{-1}). An analysis of the radial velocities of OH/IR sources also exhibits a slow rotation of the bulge (Olnon et al. 1981). Recently, an analysis of the distribution of bulge sources has shown that the

* Nobeyama Radio Observatory is a branch of the National Astronomical Observatory, an inter-university research institute operated by the Ministry of Education, Science and Culture.

Table 1. Telescope parameters for the NRO 45-m.

Frequency (GHz)	System temperature (K)	Half-power beam width (″)	Aperture efficiency	Conv. factor to flux density (Jy K^{-1})
22	200	74	0.63	2.8
43	800	41	0.49	3.6

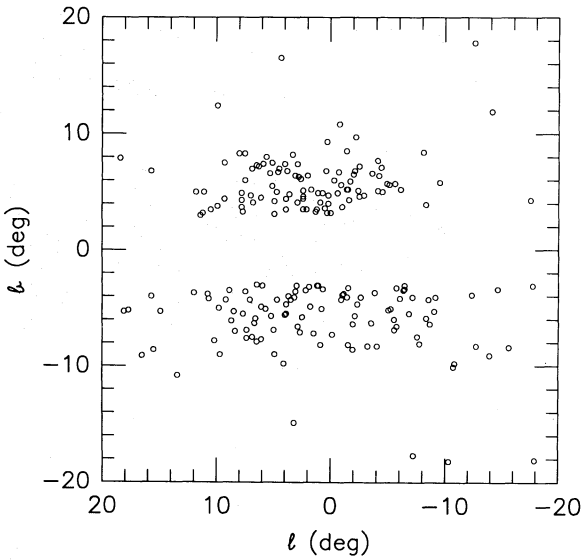

Fig. 1. Distribution of IRAS point sources based on selection conditions (a)–(d), and $|b| > 3°$. The total number of sources plotted is 204. The round shape of the bulge can be seen in the region with $|l| < 10°$ and $|b| < 8°$. Disk sources were excluded based on the condition $|b| > 3°$.

shape of the galactic bulge is bar-like (Blitz and Spergel 1991; Nakada et al. 1991).

Though to discuss bulge kinematics is not a primary purpose of this paper, we present the results of simple analysis of the rotation curve of bulge SiO maser sources that are based on the limited samples in this survey. In order to formulate an accurate rotation law of the bulge we need to observe more samples with both wider color criteria and wider search areas. We also must separate the sources that are unavoidably contaminated by the galactic disk. In the present paper, we simply mention the possibility of determining an accurate bulge rotation rate by the SiO and H_2O maser survey. An analysis based on a more extensive survey (presently being carried out) will be presented in future papers.

2. Observations

The observations based on H_2O and SiO ($J = 1$–0, $v = 2$ and 1) at 22.235 GHz, 42.820 GHz, and 43.243 GHz, respectively, were made using the Nobeyama 45-m radio telescope during 1990 January 21–25. We used a cooled high electron mobility transistor amplifier (HEMT) for the 22 GHz observation and a cooled SiS receiver for the 42 and 43 GHz observations. An acousto-optical spectrometer (AOS) having 8 arrays with 2048 channels each was used with resolutions of 40 and 250 kHz. The range of radial velocities that it covered was approximately ± 250 km s^{-1} (the effective range is determined by the band edge of the SiS receiver and by the flatness of the baseline). The telescope parameters are listed in table 1. The antenna temperature used in this paper was corrected for ohmic loss and atmospheric attenuation, but not for beam or aperture efficiency. The last column in table 1 gives the conversion factor of the antenna temperature to the flux density. The observations were made in a dual-position switching mode with a reference position offset by $\pm 5'$ in declination; two frequencies (22 and 43 GHz) were observed simultaneously (by splitting the beam into two orthogonal linear polarizations). The system temperatures, including the atmosphere, were typically 200 K at 22 GHz and 800 K at 43 GHz. The pointing was checked every two hours by nearby SiO maser sources; the average pointing error was about 5″.

The source selection was made by the following considerations. Since the distances of individual IRAS objects are not known, sources in the galactic disk can be contaminated in the samples. The map of IRAS point sources of the galactic center region indicates that samples with a certain limited range of colors and fluxes are dominated by bulge objects (Habing 1986; Rowan-Robinson and Chester 1987). The bulge stars are presumably old and their maximum luminosities do not greatly exceed 3000 $L_\odot$. A simple estimation indicates that a normal M giant ($L = 3000\ L_\odot$ and $T_{\rm eff} = 3000$ K without dust shell) would be observed as a source of 0.5 Jy at 12 μm (IRAS sensitivity limit) when it is located at 2.5 kpc. It should have a color, $(\log[f_\nu(25)/f_\nu(12)])$, of about -0.6. Dust-enshrouded objects with the same luminosity at the galactic bulge (8 kpc) should have 4.4 Jy

Table 2. Observational results for IRAS bulge sources.

IRAS sources	SiO(J = 1–0, v = 2)			SiO(J = 1–0, v = 1)			H_2O		
	T_a (K)	V_{lsr} (km s^{-1})	ΔV (km s^{-1})	T_a (K)	V_{lsr} (km s^{-1})	ΔV (km s^{-1})	T_a (K)	V_{lsr} (km s^{-1})	ΔV (km s^{-1})
17030−2801	0.53	−49.0	1.5	0.36	−48.5	2.6	...	...	...
17088−2700	0.45	8.8	1.4	...	...	...	...	...	...
17118−2952	...	...	...	...	...	...	...	...	...
17155−2546	1.48	−38.4	1.1	1.40	−36.1	1.9	0.24	−46.6	0.9
17192−2717	0.41	−155.6	3.3	0.50	−155.2	3.3	0.66(0.21)	−171.6(−139.0)	2.1(4.9)
17199−2145	0.28	−53.6	1.7	0.40	−52.6	3.0	...	...	...
17215−2228	...	...	...	...	...	...	...	...	...
17250−2615	0.30	−2.8	3.7	0.34	−2.8	1.8	0.39	−16.2	2.8
17287−1955	...	...	...	...	...	...	...	...	...
17293−1810	0.17	97.5	2.6	0.31	97.0	1.4	...	...	...
17302−2055	...	...	...	...	...	...	...	...	...
17345−2218	0.21	−53.4	3.0	...	...	...	...	...	...
17347−2459	...	...	...	...	...	...	...	...	...
17396−2122	0.79	2.8	2.9	0.68	3.8	5.6	0.28	21.8	1.4
17421−2307	0.81	37.3	3.5	1.04	37.3	1.8	1.16	24.2	1.6
17473−1839	0.31	−18.0	4.2	0.33	−19.0	3.0	...	...	...
17505−1828	...	...	...	...	...	...	...	...	...
17574−2928	0.31	−98.9	0.7	...	...	...	...	...	...
18074−2805	0.46	109.2	1.4	0.16	111.2	3.5	0.15	110.5	1.8
18154−2603	0.28	107.9	2.9	0.34	107.2	2.0	...	...	...
18209−2756	...	...	...	...	...	...	...	...	...
18264−2720	...	...	...	...	...	...	...	...	...
18287−2611	0.37	24.3	4.7	0.32	24.3	1.4	...	...	...

at 12 μm for T_{eff} = 300 K (the color is 0.0) and 0.8 Jy at 12 μm for T_{eff} = 1000 K (a color of −0.4).

The above considerations suggest that we should see mostly bulge sources with an IRAS color of $\sim$ 0 and fluxes of around 5 Jy at 12 μm. After inspecting the sky maps for IRAS point sources selected by various criteria, we found that the following conditions are suitable for extracting the bulge sources from the IRAS Point Source Catalog:

(a) high or good measurement quality at 12, 25, and 60 μm,

(b) $\log[f_\nu(60)/f_\nu(25)] \sim -0.6$,

(c) $0 < \log[f_\nu(25)/f_\nu(12)] < 0.2$,

(d) $f_\nu(12) < 14$ Jy,

(e) $|l| < 10°$,

(f) $3° < |b| < 10°$, and

(g) $\delta > -30°$.

Condition (f) excludes areas near to the Galactic plane, rejecting contamination of the disk sources. Condition (g) was added in order to secure observations at Nobeyama in the northern hemisphere. The validity of our selection criterion can be checked by mapping the selected sources. Figure 1 shows the distribution of the 204 IRAS sources with selection conditions (a), (b), (c), (d), and $|b| > 3°$. Apparently, it exhibits a well-defined shape of the bulge, extending from $l = -10°$ to 10° and from $b = -8°$ to 8°, thus supporting the belief that our criterion preferentially selects bulge sources. There still remain many sources which were rejected by our criterion. It is difficult to judge whether these rejected sources belong to the bulge or to the foreground disk.

Among the 121 sources which satisfy the above-mentioned criterion, the brightest 23 sources were selected for observation. The observational results are summarized in table 2. The peak antenna temperature, the radial velocities and the full line width at the half maximum are shown for each transition. The sign "..." indicates non-detection. The spectra are shown in figures 2a–o. The rms noise level in the spectra was typically 0.06 K at 22 GHz and 0.14 K at 43 GHz.

Table 3. Properties of IRAS bulge sources.

IRAS sources	Galactic coordinates l (°)	b (°)	IRAS data $f_\nu(12)$ (Jy)	25/12	60/25	OH 1612 MHz V_{lsr} (km s^{-1})	ΔV (km s^{-1})	Period (d)
17030−2801	−4.1	7.7	9.6	0.13	−0.55			722
17088−2700	−2.5	7.2	13.1	0.14	−0.49	−7.5	...	...
17118−2952	−4.5	5.0	7.7	0.18	−0.38	−41.0	28.3	
17155−2546	−0.7	6.7	13.9	0.99	−0.52	−35.4	33.6	
17192−2717	−1.4	5.2	7.9	0.14	−0.65			
17199−2145	3.3	8.2	11.2	0.02	−0.67			
17215−2228	2.9	7.4	10.6	0.10	−0.77			...
17250−2615	0.2	4.7	7.5	0.03	−0.62			
17287−1955	5.9	7.4	8.3	0.17	−0.62			578
17293−1810	7.5	8.3	6.2	0.09	−0.60			
17302−2055	5.3	6.6	10.4	0.03	−0.64			
17345−2218	4.7	5.0	9.0	0.06	−0.62	−54.3	29.1	
17347−2459	2.4	3.5	8.0	0.19	−0.89			
17396−2122	6.1	4.5	9.9	0.01	−1.10			
17421−2307	4.9	3.1	11.8	0.01	−1.03			
17473−1839	9.3	4.4	8.0	0.03	−0.73			
17505−1828	9.9	3.8	8.3	0.04	−0.74			
17574−2928	1.2	−3.1	10.1	0.07	−0.60	−98.7	29.8	
18074−2805	3.5	−4.3	9.1	0.10	−0.79			
18154−2603	6.1	−4.9	8.0	0.03	−0.54			
18209−2756	5.0	−6.9	8.9	0.04	−0.58			
18264−2720	6.1	−7.7	8.7	0.02	−0.68			660
18287−2611	7.4	−7.6	8.6	0.11	−0.66			666

3. Maser Properties

The infrared properties of the bulge sources are summarized in table 3. The 5th and 6th columns (indicated by 25/12 and 60/25) are colors $\log[f_\nu(25)/f_\nu(12)]$ and $\log[f_\nu(60)/f_\nu(25)]$, respectively. The OH 1612 MHz maser were previously detected in 5 sources in these samples by te Lintel-Hekkert (1990). Near-infrared $JHKL$ photometric observations were made by Whitelock et al. (1991), and the period of intensity variation was determined for 4 sources among these samples. These data are also included in table 3. The OH 1612 MHz spectra from late-type stars are known to exhibit double-peaks, which are emitted from approaching and receding parts of the expanding shell. The center velocity and the velocity separation of the two peaks are listed in table 3. The radial velocities of SiO masers for bulge sources fall between the two OH double-peak velocities. It is well known that the radial velocity of SiO masers coincides with the stellar velocity (on average) whithin an accuracy of a few km s^{-1} (Jewell et al. 1991).

3.1. *SiO Maser Intensity*

Emission from the SiO $J = 1$–0, $v = 2$ transition was detected in 15 out of the 23 sources searched. The number of detected sources for the $J = 1$–0, $v = 1$ transition was 12. The detection rates (65% and 52% for $v = 2$ and $v = 1$, respectively) seem high, especially when we consider the large distance of 8 kpc and the presumably small mass of the bulge stars. We suspect that the bulge sources are unusually strong maser emitters.

The peak flux density of the SiO masers observed in the present study ranged from 5.3 to 0.7 Jy. Bujarrabal et al. (1987) and Alcolea et al. (1990) have found a linear relation between the peak maser flux density [f_ν (SiO $J = 1$–0, $v = 1$)], and the continuum flux at mid-infrared wavelengths (at the light maximum of Mira variables). According to them, the highest correlation with the maser intensity was found for the continuum flux density at 8 μm as f_ν(SiO, $J = 1$–0, $v = 1$)= 0.2 f_ν (8 μm) for disk stars. We checked this relation for bulge SiO maser sources. (Here, we used the peak flux density instead of the flux of SiO masers, since we felt that the line widths for the weak sources were almost determined by the noise in the spectrometer.) Because the continuum flux density at 8 μm is, unfortunately, not available for these bulge stars, we used the corrected 8 μm intensity, which was computed from the IRAS 12 μm intensity with a logarithmic correction factor of −0.06. The correction

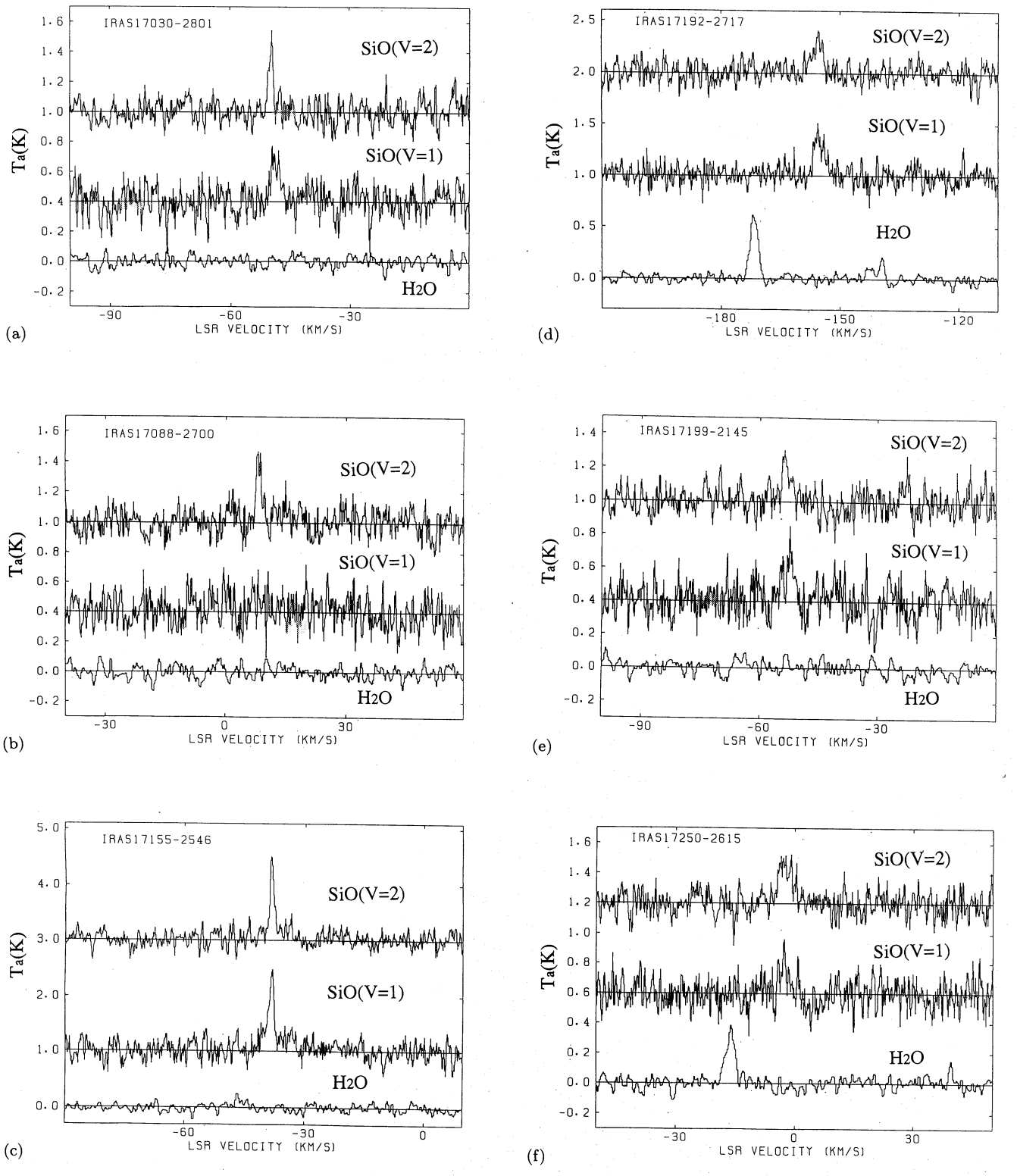

Fig. 2. Spectra of the SiO $J = 1$–0, $v = 2$ (top) and $v = 1$ line (middle) and H_2O 6_{16}-5_{23} line (bottom) for bulge sources. The spectra for 15 detected sources are shown in pannels (a)–(o).

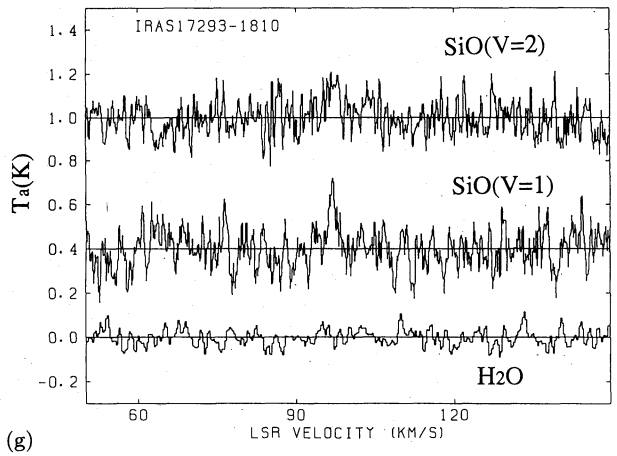

(g)

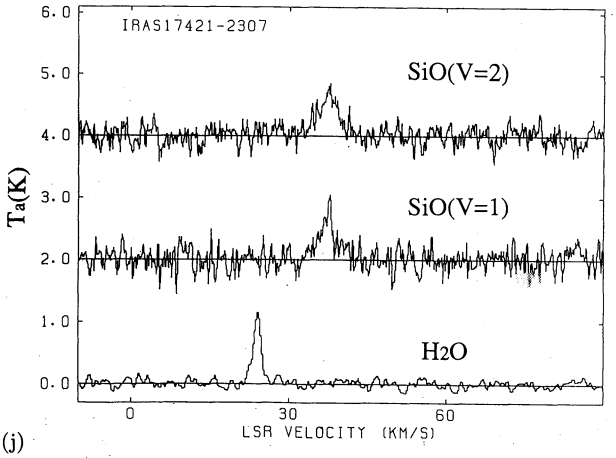

(j)

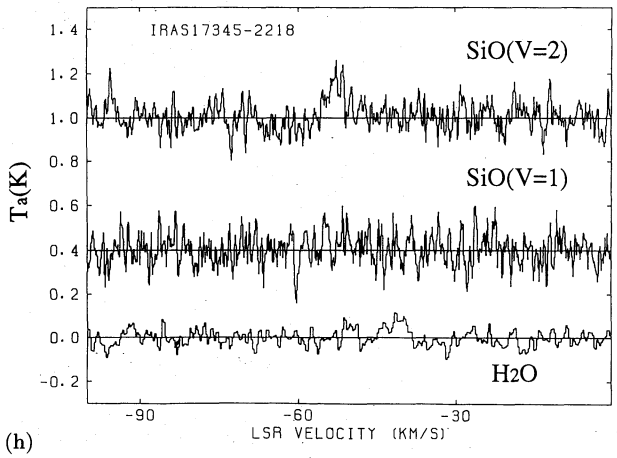

(h)

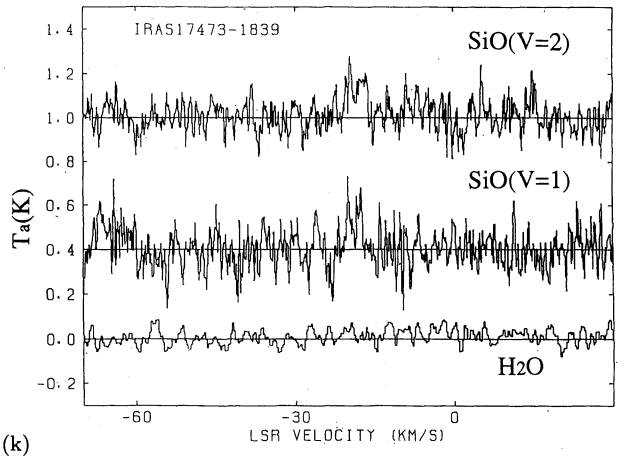

(k)

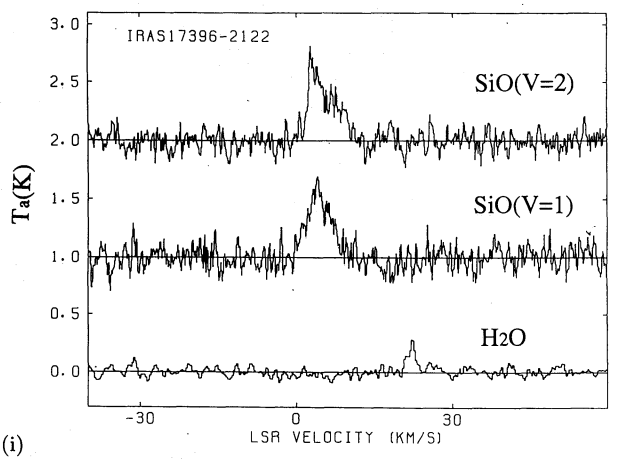

(i)

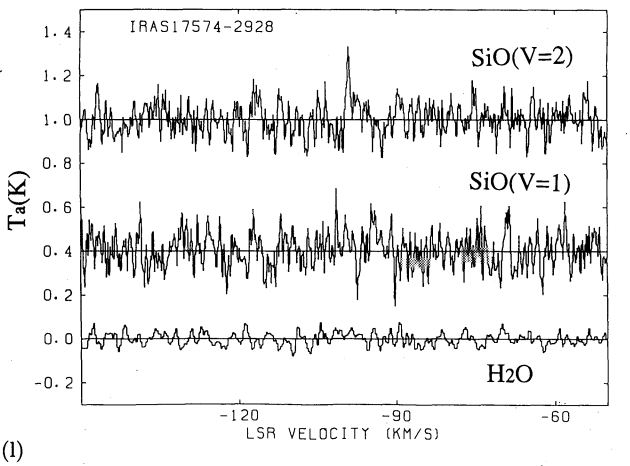

(l)

Fig. 2. (Continued)

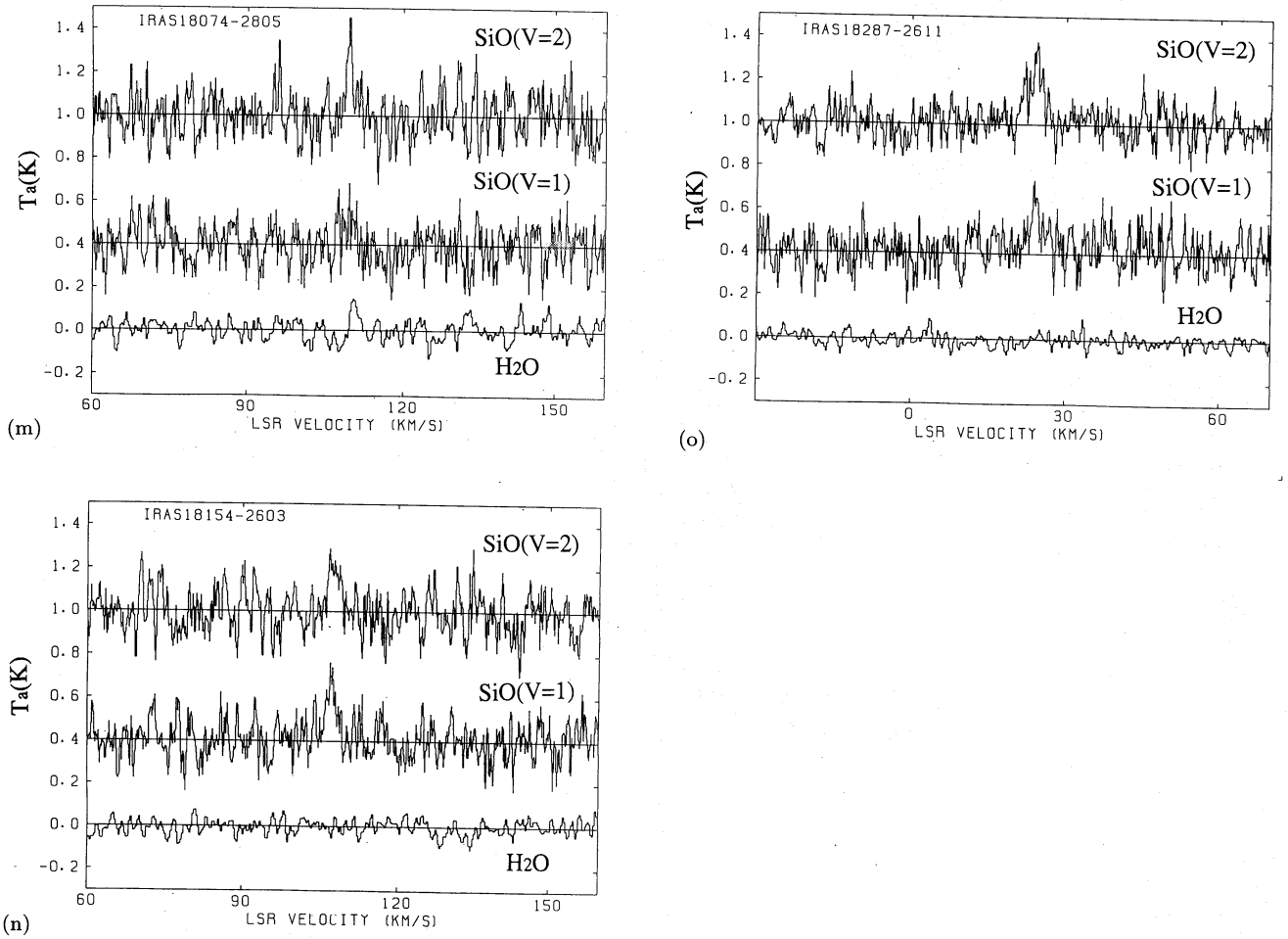

Fig. 2. (Continued)

factor was deduced from normal disk infrared objects based on the assumption that the infrared spectra for both bulge and disk sources are similar. Since the color, $(\log[f_\nu(25)/f_\nu(12)])$, was between 0.0 and 0.2 for the selected sources, the 8 μm flux density is slightly smaller than the 12 μm flux density on the average. The absolute flux densities at the SiO wavelength (7 mm) and at 8 μm were obtained using $F_\nu = f_\nu(d/10\ \mathrm{pc})^2$, where the distance to the source, (d), is assumed to be 8 kpc. They are plotted in figure 3, together with disk Miras and disk supergiants (taken from Bujarrabal et al. 1987). The bulge sources lie along the line between the disk Miras and disk supergiants. This fact suggests that the bulge SiO masers are very similar to the disk SiO masers, and that the maser pump mechanism is similar in both sources. The area occupied by bulge sources in figure 3 is near to the middle between the disk Miras and disk supergiants.

Figure 3 indicates that the bulge IRAS sources are not unusually strong maser emitters. The high detection rate of SiO masers in this survey is probably due to the high sensitivity of the 45-m radio telescope at Nobeyama at the observed frequencies. The simultaneous observation by two transitions of SiO $J = 1$–0 $v = 1$ and 2 also makes the identification of the signals from noises easier, leading to the high detection rate for SiO masers.

3.2. Time Variation

The time variations of the SiO masers have been found for Miras, semi-regulars, and supergiants (Nyman et al. 1986; Gómez-Balboa and Lépine 1986). A phase lag of about 0.–0.2 to the infrared variability has been reported (Martínez et al. 1988). The ratio of the maximum-to-minimum flux varies from 3 to 9, increasing with the amplitude of the infrared continuum variation. The IRAS variability index for these maser sources is greater than 93 in most cases, thus indicating a high probability of time variation at infrared wavelengths. Whitelock et al. (1991) carried out near-infrared photometric observa-

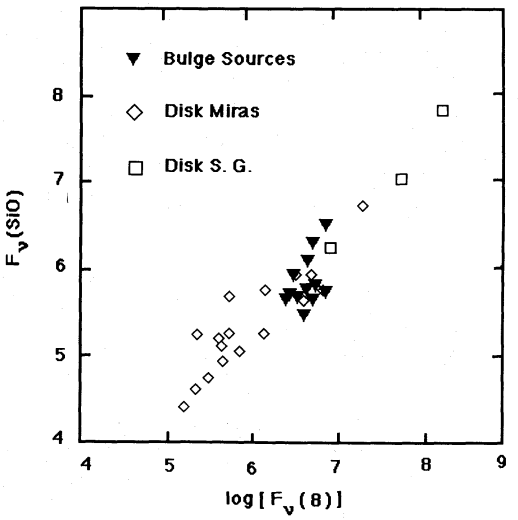

Fig. 3. Peak intensity of the SiO $J = 1$–0, $v = 1$ maser emission versus the infrared intensity for the bulge IRAS sources (filled triangles) and the disk Miras (diamonds) and disk supergiants (squares). Both intensities are normalized at the distance of 10 pc.

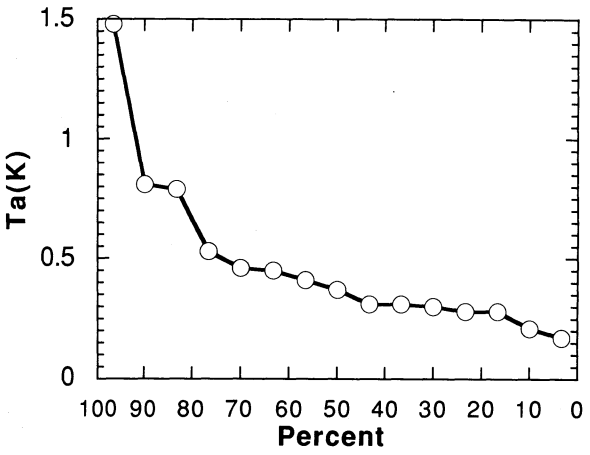

Fig. 4. Number-peak intensity (SiO $J = 1$–0, $v = 2$ masers) relation. This curve is considered to simulate the time variation of a single maser.

tions of the 141 bulge IRAS sources and determined the period of intensity variations at the $JHKL$ bands. In the bulge sources given in table 3, 6 sources were observed by them; the period of these sources is in the range between 578–722 d. They seem to belong to the longest-period Mira group among these bulge variable sources. This is probably due to the color selection effect for the sources that we chose. Though no monitoring observation was made for the bulge SiO masers, strong time variations with a period of about two years are usually expected.

The bulge sources that we observed comprise a rather homogeneous group in terms of infrared fluxes and colors. In order to obtain a rough idea of the time variability of the bulge masers, we assumed that the observed bulge sources had a similar light curves, but were observed randomly at different phases of a period. The frequency distribution of the maser fluxes was thus considered to roughly simulate the flux variation distribution of a single maser. Figure 4 shows such a frequency distribution of the maser intensity for the 15 sources detected. We note that the distribution of intensities given in figure 4 looks like the light curves of the maser intensity from a Mira variable (i.e., Martínez et al. 1988). The suggested ratio of the maximum-to-minimum intensity is greater than 9, which is near to the upper limit of the disk Mira variation. One of the disk-source SiO surveys (Jewell et al. 1985) reported 20 detections by the SiO $J = 1$–0, $v = 1$ transition out of 50 OH/IR sources, concluding that the SiO maser is quite common among these stars. The same conclusion could be applied to bulge IRAS sources. Further, it is well known that bulge infrared sources are mostly M-type stars but rarely C-type stars (Frogel 1988). We can thus say that a non-detection of SiO masers is simply due to the time variation.

However, despite the homogeneity of the samples that we have chosen, it is not certain whether the SiO maser property is also similar to each other for the observed sources or not. The previous monitoring of SiO masers from disk Miras suggests that the maximum intensity and amplitude of the light curve vary from cycle to cycle and from source to source (Nyman and Olofsson 1986). Further monitoring observations will tell if all of the IRAS bulge sources with a certain infrared color exhibit SiO maser emission or not.

3.3. *Intensity Ratio of the J=1–0, v=2 to the J=1–0, v=1 Line*

We have simultaneously observed two transitions of SiO, $J = 1$–0, $v = 1$ and 2. The radial velocities of emission for $v = 1$ coincide well with that of $v = 2$. In most cases, they coincide with each other with a difference of less than 1 km s^{-1}. It is, therefore, strongly suggested that both emissions emerge from the same area within the circumstellar envelope. We have found that the ratio of the SiO $v = 1$ to $v = 2$ peak intensity scatters between 0.7 to 1.3. Observations of the disk Miras (Schwartz et al. 1979; Spencer et al. 1981) have shown that this ratio is nearly 1. Nyman et al. (1986) have suggested that this ratio is higher for OH/IR sources (about 4). The high ratio for OH/IR sources might be explained by the sensitive response of the $v = 2$ level populations to the infrared fluxes.

The bulge IRAS sources which we selected have colors that are similar to the colors of luminous Miras (see fig-

ure 3). If the infrared continuum spectrum controls the maser intensity ratio, we expect that an intensity ratio of $v = 2$ to $v = 1$ is around 1 for the bulge sources, which is quite consistent with the present observations. According to the standard theory (Langer and Watson 1984), the intensity ratio of the $v = 2$ maser to $v = 1$ is mainly determined by the shape of the infrared spectrum (at 4 and 8 μm), which is different between an OH/IR source and Miras. The near-infrared colors and band strengths of the bulge late-type stars (non-variable M stars) are slightly different from those of disk stars (Frogel and Whitford 1987). The small difference in the colors is attributed to the bulge star population with a metalicity that is in considerable excess of the solar values. The observed intensity ratio is consistent with the fact that the bulge sources are very similar to disk Miras. We conclude that the color differences of the bulge sources from disk Miras do not influence the SiO intensity ratio.

3.4. H_2O Maser

Water maser emission has been found in six sources out of the 23 objects searched. The peak intensity ranges from 0.4 to 3.2 Jy. The detection rate of 26 % is comparable with that of 24% for the H_2O maser survey for the disk IRAS sources at Parkes (Deguchi et al. 1989). The radial velocity of the H_2O emission is randomly shifted by 5 to 20 km s^{-1} from the radial velocity of SiO masers for IRAS 17155−2546 (figure 2c), and IRAS 17250−2615 (figure 2f), and IRAS 17421−2307 (figure 2j). The H_2O spectrum of IRAS 17192−2717 (figure 2d) exhibits double peaks, and the center velocity of the two peaks (155.3 km s^{-1}) agrees well with the radial velocity of SiO emission. The double peaks probably come from the approaching and receding parts of the expanding shell. The expanding velocity of the shell of this star is thus about 16.3 km s^{-1}. It also suggests that although the blue- or red-shifted peaks of the former three sources are a part of the pairs, another component is missing for some reason. On the other hand, emission for IRAS 18074−2805 (figure 2m) appears at the same velocity as the SiO velocity.

These properties of the radial velocity difference between H_2O and SiO masers are consistent with former studies involving disk late-type stars. Engels et al. (1986, 1988) investigated the radial velocities of OH, H_2O, and SiO masers in late-type stars and OH/IR sources, finding that H_2O masers normally have double peaks with a velocity separation that is slightly smaller than the separation of the OH 1612 MHz double peaks in most cases. In some cases, however, the complex of emission falls at the center of the OH double peaks (Engels et al. 1986).

Although the number of detected H_2O masers was small in this survey, the observed properties of H_2O masers in bulge stars was quite similar to the properties of disk H_2O masers.

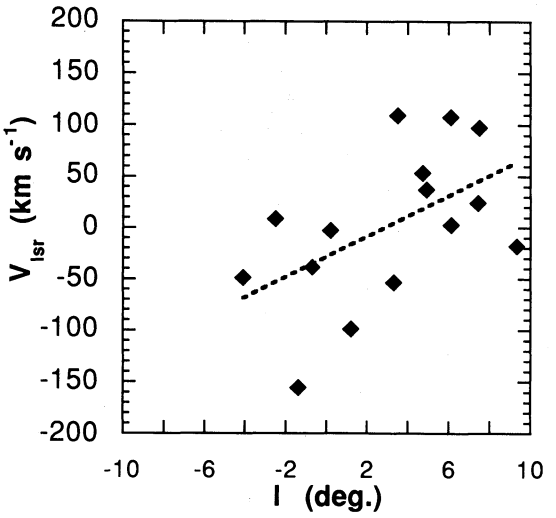

Fig. 5. Radial velocity-galactic longitude plot. The filled diamonds are the data points for 15 sources. The broken line is the best linear fit to the observational data [$V_{lsr} = -28.4 + 9.9\ (l/\mathrm{deg})$ km s^{-1}].

4. Rotation of the Galactic Bulge

To examine bulge kinematics, we plotted the radial velocities of SiO masers versus the galactic longitude (figure 5). The premise of this analysis was that the SiO maser velocity represents the stellar velocity. As discussed in the previous section, this is approximately satisfied to an accuracy of about a few km s^{-1}. The data given in figure 5 show a systematic change in the radial velocity with the galactic longitude, suggesting that the galactic bulge is rotating. A simple linear fit to the data points gives a rotation rate of 9.9 (±2.2) km s^{-1} deg^{-1} between $l = -5°$ to 10° [the best fit is $V_{lsr} = -28.4 + 9.9(l/\mathrm{deg})$ km s^{-1}]. A large random motion with a dispersion of about 70 km s^{-1} can also be seen in figure 5. The linear-fit rotation rate is actually that obtained by averaging over the star velocities along the line of sight. It expresses the systematic motion approximated by solid-body rotation.

It should be noted that the distribution of 15 samples is not very uniform with respect to the galactic longitudes and latitudes. These are rather concentrated at the first quadrant of the $l - b$ plane (due to the observational constraint at Nobeyama). The most probable value of V_{lsr} at $l = 0$ deviates from zero, probably because of this effect.

Minkowski (1964) first pointed out that the central subsystem of planetary nebulae rotates more slowly than

does a flat disk. Although similar results were obtained for the Miras (Feast 1966, 1972; Feast et al. 1980), subsequent observations in Baade's window did not confirm the systematic rotation of the bulge. Gratton (1987) determined the systematic velocity of 11 ± 34 km s^{-1} for the 17 RR Lyrae stars in Baade's window, while Mould (1983) observed 50 M stars in this region to obtain a mean velocity of -10 ± 19 km s^{-1}. Based on an analysis of the radial velocity of OH/IR stars in the bulge, Olnon et al. (1981) also concluded that little evidence exists for bulge rotation. Isaacman and Oort (1981) took the same view when they constructed mass model of the galactic bulge without rotation. In another extreme, Habing et al. (1983) obtained a rotation rate of 200 km s^{-1} deg^{-1} based on the radial velocities of OH/IR stars within 1° of the galactic center. However, recent studies suggest a moderate rotation. For example, Kinman et al. (1988) derived a rotation rate of 12 ± 1.9 km s^{-1} deg^{-1} for bulge planetary nebulae. Menzies (1990) obtained rotation rate of 9.8 ± 1.9 km s^{-1} deg^{-1} for the 26 Miras from the Whitelock et al. (1991)'s samples. Minniti et al. (1992) obtained the rotational rate of about 7 km s^{-1} deg^{-1} from the spectroscopic observations of K giants.

Although we only had 15 samples, our data clearly show a slow rotation of the galactic bulge with a rate of 10 km s^{-1} deg^{-1}. This value is consistent with those previously obtained from optical observations. An analysis using more samples will be presented in subsequent papers. Here, we conclude that SiO masers have been proved to be an excellent tool for studying the rotation of the galactic bulge.

5. Summary

We observed 23 IRAS objects in the galactic bulge using H_2O and SiO lines, and detected the SiO $J = 1$–0, $v = 2$ transition in 15 sources, the SiO $J = 1$–0, $v = 1$ transition in 12 sources, and the H_2O 6_{16}–5_{23} transition in 6 sources. The SiO maser properties, i.e., maser luminosities, for the bulge sources are very similar to those of disk Miras. The relative strength of the SiO $v = 2$ line to the $v = 1$ line is close to the value of disk Miras, and apparently, lower than the values for disk OH/IR sources with similar colors. SiO masers have been proved to be one of the best tools for measuring the rotation of the Galactic bulge.

Y. N. thanks Dr. M. Feast for helpful discussions. He also thanks the staff of Nobeyama Radio observatory for their cooperation. This research was supported by a Scientific Research Grant of the Ministry of Education, Science and Culture (No. 03640244C).

References

Alcolea, J., Bujarrabal, V., and Gómez-Gonzáles, J. 1990, *Astron. Astrophys.*, **231**, 431.
Blitz, L., and Spergel, D. N. 1991, *Astrophys. J.*, **379**, 631.
Bujarrabal, V., Planesas, P., and del Romero, A. 1987, *Astron. Astrophys.*, **175**, 164.
Deguchi, S., Nakada, Y., Forster, R. 1989, *Monthly Notices Roy. Astron. Soc.*, **132**, 495.
Engels, D., Schmidt-Burgk, J., and Walmsley, C. M. 1986, *Astron. Astrophys.*, **167**, 129.
Engels, D., Schmidt-Burgk, J., and Walmsley, C. M. 1988, *Astron. Astrophys.*, **191**, 283.
Feast, M. W. 1966, *Monthly Notices Roy. Astron. Soc.*, **132**, 495.
Feast, M. W. 1972, *Vistas Astron.*, **13**, 207.
Feast, M. W. 1987, in *The Galaxy*, ed. G. Gilmore and B. Carswell (D. Reidel Publishing Company, Dordrecht), p. 1.
Feast, M. W., Robertson, B. S. C., and Black, C. 1980, *Monthly Notices Roy Astron. Soc.*, **190**, 227.
Frogel, J. A. 1988, *Ann. Rev. Astron. Astrophys.*, **26**, 51.
Frogel, J. A., and Whitford, A. E. 1987, *Astrophys. J.*, **320**, 199.
Gómez-Balbora, A. M., and Lépine, J. D. R. 1986, *Astron. Astrophys.*, **159**, 166.
Gratton, R. G. 1987, *Monthly Notices Roy. Astron. Soc.*, **224**, 175.
Habing, H. J. 1986, in *Light on Dark Matter, Proc. 1st IRAS Conf.*, ed. F. P. Israel (D. Reidel Publishing Company, Dordrecht), p. 329.
Habing, H. J., Olnon, F. M., Winnberg, A., Matthews, H. E., and Baud, B. 1983, *Astron. Astrophys.*, **128**, 230.
Heske, A. 1987, in *Circumstellar Matter, IAU Symp. No. 122*, ed. I. Appenzeller and C. Jordan (D. Reidel Publishing Company, Dordrecht), p. 253.
Isaacman, R., and Oort, M. J. A. 1981, *Astron. Astrophys.*, **102**, 347.
Jewell, P. R., Snyder, L. E., Walmsley, C. M., Wilson, T. L., and Gensheimer, P. D. 1991, *Astron. Astrophys.*, **242**, 211.
Jewell, P. R., Walmsley, C. M., Wilson, T. L., and Snyder, L. E. 1985, *Astrophys. J. Letters*, **298**, L55.
Kinman, T. D., Feast, M. W., and Lasker, B. M. 1988, *Astron. J.*, **95**, 804.
Langer, S. H., and Watson, W. D. 1984, *Astrophys. J.*, **284**, 751.
Martínez, A., Bujarrabal, V., and Alcorea, J. 1988, *Astron. Astrophys. Suppl.*, **74**, 273.
Menzies, J. W. 1990, in *Bulges of Galaxies, ESO-CTIO Workshop*, ed. B. J. Javis and D. M. Turndrup, p. 115.
Minkowski, R. 1964, *Publ. Astron. Soc. Pacific.*, **76**, 197.
Minniti, D., White, S. D. M., Olzszewski, E. W., and Hill, J. M. 1992, *Astrophys. J. Letters*, **393**, L47.
Mould, J. R. 1983, *Astrophys. J.*, **266**, 255.
Nakada, Y., Deguchi, S., Hashimoto, O., Izumiura, H., Onaka, T., Sekiguchi, K., and Yamamura, I. 1991, *Nature*, **353**, 140.
Nyman, L.-Å., Johansson, L. F. B., and Booth, R. S. 1986, *Astron. Astrophys.*, **160**, 352.

Nyman, L.-Å., and Olofsson, H. 1986, *Astron. Astrophys.*, **158**, 67.
Olnon, F. M., Walterbos, R. A. M., Habing, H. J., Matthews, H. E., Winnberg, A., Brzezinska, H., and Baud, B. 1981, *Astrophys. J. Letters*, **245**, L103.
Reid, M. J., Schneps, M. H., Moran, J. M., Gwinn, C. R., Genzel, R., Downes, D., and Rönnäng, B. 1988, *Astrophys. J.*, **330**, 809.
Rowan-Robinson, M., and Chester, T. 1987, *Astrophys. J.*, **313**, 413.
Schwartz, P. R., Waak, J. A., and Bologna, J. M. 1979, *Astron. J.*, **84**, 1349.
Spencer, J. H., Winnberg, A., Olnon, F. M., Schwartz, P. R., Matthews, H. E., and Downes, D. 1981, *Astron. J.*, **86**, 392.
te Lintel-Hekkert, P. 1990, Ph. D. Thesis, Leiden Univeristy.
Whitelock, P., Feast, M., and Catchpole, R. 1991, *Monthly Notices Roy. Astron. Soc.*, **248**, 276.